Ocean Engineering 129 (2017) 389–400

Contents lists available at ScienceDirect

Ocean Engineering

journal homepage: www.elsevier.com/locate/oceaneng

Robust Dynamic Positioning of offshore vessels using mixed-μ synthesis modeling, design, and practice☆

Vahid Hassani[a,b,c,*], Asgeir J. Sørensen[c,d], António M. Pascoal[a], Michael Athans[a,1]

[a] Institute for Systems and Robotics (ISR/IST), LARSyS, Instituto Superior Técnico, University of Lisboa, Portugal
[b] Norwegian Marine Technology Research Institute (MARINTEK), Trondheim, Norway
[c] Department of Marine Technology, Norwegian University of Science and Technology, Trondheim, Norway
[d] Centre for Autonomous Marine Operations and Systems (AMOS), Trondheim, Norway

ARTICLE INFO

Keywords:
Dynamic Positioning
Offshore vessel modelling
Robust control

ABSTRACT

This paper describes a procedure to design robust controllers for Dynamic Positioning (DP) of ships and offshore rigs subjected to the influence of sea waves, currents, and wind loads using $\mathcal{H}_\infty$ and mixed-μ techniques. The proposed method will increase operational weather window and robustness of the DP vessel and associated DP system. To this effect, practical assumptions are exploited in order to obtain a linear design model with parametric uncertainties describing the dynamics of the vessel. Appropriate frequency weighting functions are selected to capture the required performance specifications at the controller design phase. The proposed model and weighting functions are then used to design robust controllers. The problem of wave filtering is also addressed during the process of modelling and controller design. The key contribution of the paper is threefold: (i) it affords system designers a new method to efficiently obtain linearized design models that fit naturally in the framework of $\mathcal{H}_\infty$ control theory, (ii) it describes, in a systematic manner, the different steps involved in the controller design process for DP systems operating under different sea conditions, and (iii) it contains the details of simulations and results of experimental model tests in a towing tank equipped with a hydraulic wave maker.

1. Introduction

The advent of offshore exploration and exploitation at an unprecedented scale has brought about increasing interest in the development of Dynamic Positioning (DP) systems for surface vessels. Currently, there are more than 2000 DP vessels of various kinds operating worldwide, see Sørensen (2011a). DP systems are used with a wide range of vessel types and in different marine operations; in particular, in the offshore, oil, and gas industries many applications are only possible with the use of DP systems for service vessels, drilling rigs and ships, shuttle tankers, cable and pipe layers, floating production offloading and storage units (FPSOs), crane and heavy lift vessels, geological survey vessels, and multi-purpose vessels. Most of the offshore operations, such as cable and pipe laying, do also need tracking functionality. The main purpose of DP systems is to keep the position and heading of marine structures within pre-specified excursion limits under expected weather windows. As such, they play a key role in many offshore operations aimed at improving the efficiency and safety of the particular operation. DP systems came to existence in the 1960s for offshore drilling applications for the first time, due to the need to drill in deep waters and the realization that Jack-up barges and anchoring systems could not be used economically at such depths. Early DP systems were implemented using PID controllers, and in order to restrain thruster trembling caused by the wave-induced motion components, notch filters in cascade with low pass filters were used with the controllers. However, notch filters restrict the performance of closed-loop systems because they introduce some phase lag around the crossover frequency, which in turn tends to decrease the phase margin. An improvement in performance was achieved by exploiting more advanced control techniques based on optimal control and Kalman filter theory, see Balchen et al. (1976). All these techniques were later modified and extended in Balchen et al. (1980), Grimble

☆ This work was supported in part by FCT [UID/EEA/50009/2013] and the European Commission under the H2020-ICT-2014 WiMUST Project (Grant Agreement No. 645141) and was carried out in cooperation with the Centre for Autonomous Marine Operations and Systems (AMOS) and the Norwegian Marine Technology Research Institute (MARINTEK); the Norwegian Research Council is acknowledged as the main sponsor of AMOS.

* Corresponding author at: Department of Marine Technology, Norwegian University of Science and Technology, Trondheim, Norway.
E-mail addresses: vahid.hassani@ntnu.no (V. Hassani), asgeir.sorensen@ntnu.no (A.J. Sørensen), antonio@isr.ist.utl.pt (A.M. Pascoal), athans@isr.ist.utl.pt (M. Athans).
[1] Michael Athans is also Professor of EECS (emeritus), M.I.T., USA.

http://dx.doi.org/10.1016/j.oceaneng.2016.10.041
Received 17 June 2015; Received in revised form 18 October 2016; Accepted 22 October 2016
Available online 06 December 2016

et al. (1980a,b), Fung and Grimble (1983), Sælid et al. (1983), Fossen et al. (1996), Sørensen et al. (1996), and Fossen and Perez (2009a). Applying the LQG to the problem of DP requires the linearization of the dynamics and kinematics of the plant over different operating points; besides, for each operating point a set of variables (such as covariances of disturbances and weighting matrices) needs to be computed which makes the procedure of tuning the controllers costly and burdensome. Moreover, Doyle (1978) showed that LQG has no guaranteed phase and gain margins and the resulting closed-loop regulator may have arbitrarily small stability margins. This led to the development of a simpler setup using passive observers and nonlinear multivariate PID controllers; see Fossen and Strand (1999), Strand and Fossen (1999), Strand (1999), Torsetnes et al. (2004), and Fossen (2000). The literature on ship DP is vast and defies a simple summary. See for example Sørensen (2005, 2011b) and the references therein for a short presentation of the subject and its historical evolution.

Different sources of uncertainty in the DP problem led to the application of robust control techniques to DP, see Katebi et al. (1997, 2001), Donha and Katebi (2007), Donha et al. (1997), Martin et al. (2000), Hassani et al. (2012b,c, 2013c). The $\mathcal{H}_\infty$ and mixed-μ are model-based techniques and design of a DP controller based on these methodologies requires a linear model of the plant (computed by linearization of the plant about an operating point). The computation of the latter for different operating points is cumbersome, requires intensive computations, and may be very costly. For these reasons, and in spite of the potential benefits of using robust DP controllers, the assessment of their performance has, to the best of our knowledge, been carried out using only simulations or by performing experimental tank tests; see Katebi et al. (2001).

DP systems have generally been designed for low-speed and low Froude number applications, where the basic DP functionality is either to keep a fixed position and heading of a ship, or to move it slowly from one location to another. In this work, using the low speed assumption, a linear model with parametric uncertainties is developed based on which, by assigning appropriate frequency weighting functions and using $\mathcal{H}_\infty$ and mixed-μ techniques, robust controllers for station keeping in different sea conditions (calm, moderate, high, and extreme seas) are designed. For a representative vessel, we apply the presented methodology to design robust controllers for different sea conditions and we present the discussion of the results of numerical simulations and experimental model-testing of a set of robust DP controllers operating under different sea conditions. The robust DP controllers were first evaluated in a high fidelity nonlinear DP simulator, illustrating the efficiency of the design. To bridge the gap between theory and practice, the results were experimentally verified by model testing of a DP operated ship, the CybershipIII, under different sea conditions in a model test tank with a hydraulic wave maker at the Marine Cybernetics Laboratory (MCLab) at the Department of Marine Technology, the Norwegian University of Science and Technology.

The structure of the paper is as follows. A brief introduction to important issues that arise in DP is presented in Section 2. Section 3 proposes a linear representative vessel model with parametric uncertainties. Section 4 summarizes the main ideas behind the DP robust controller designing process in calm to high sea conditions. Section 5 explains the DP controller design procedure in extreme sea conditions. Section 6 introduces the frequency weighting functions for different sea conditions; it also describes and compares the robust controllers designed for different sea conditions following the methodology proposed in this paper. In Section 7 a brief description of the Marine Cybernetics Simulator (MCSim) and the results of numerical Monte-Carlo simulations are presented. In Section 8, a short description of the model-test vessel, CybershipIII, and experimental results of model-tests are presented. Conclusions and suggestions for future research are summarized in Section 9.

2. Dynamic Positioning and wave filtering

In order to design a robust DP controller a linear model of plant must be derived first. Here, we should stress that in the marine control literature different mathematical models with different complexity levels are used for different purposes. Two important models (see Sørensen, 2011a) are formulated as the control plant model (or design plant model) and the process plant model (or simulation model). The first is a simplified mathematical description containing only the main physical properties of the process or plant and is used for the purpose of controller design and stability analysis, using for example Lyapunov stability and passivity tools. The second is a comprehensive description of the actual process whose main purpose is to simulate the real plant dynamics and is used in numerical performance and robustness analysis and testing of the control systems designed. In Section 3, we formulate the problem of modelling a DP system using a low speed assumption. A linear plant model with parametric uncertainty is obtained and used for DP controller system design. Later on, in Section 7, in order to evaluate the performance of the designed controllers, a nonlinear high fidelity model, the Marine Cybernetics Simulator (MCSim), is used.

In DP applications in open waters, waves produce a pressure change on the hull surface of the vessel. This change of pressure induces different forces and torques on the vessel. Usually, only first and second order effects of these pressure-induced forces are studied in DP applications. The first order effect of the waves has an oscillatory nature that depends linearly on the wave elevation. Hence, these forces have the same frequency as that of the waves and are therefore referred to as wave-frequency forces. The second order effect of the waves depends nonlinearly on the wave elevation, see Faltinsen (1990). The nonlinear component of wave forces is due to the quadratic dependence of the pressure on the fluid-particle velocity induced by the passing of the waves. They have a wider frequency range and they excite the vessel not only in the wave frequency range but also in lower and higher frequency ranges. While the mean wave forces make the vessel drift, the oscillatory components of the wave forces can lead to resonance in the horizontal motion of vessel under positioning control. Hence, the motions of marine vessels can often be divided into a low-frequency (LF) part and a wave-frequency (WF) part. For most positioning applications (usually for calm, moderate and high sea), only the slowly varying wave disturbances and mean wave loads (in addition to wind and current loads) should be counterbalanced by the propulsion system, whereas the oscillatory motion induced by the waves (1st-order wave effect) should not enter the feedback control loop. The reasons for this could be that either the WF motion does not matter for the particular operation or the vessel does not have enough power and thrust capacity for doing any noticeable compensation at all. The latter reason is of great importance, for there is no point in wasting fuel and cause additional wear and tear of the propulsion equipment. To this effect, the DP control systems should be designed so as to react to the LF forces on the vessel only. In the literature, this task is accomplished by using the so-called wave filtering techniques, which separate the position and heading measurements into LF and WF position and heading estimates; see Fossen (2011), and Hassani et al. (2013a,b). Wave filtering observers provide an estimate of the LF motions and velocities computed from noisy measurements of position and heading. Later, these estimates are used for control purposes. As proposed in this work, in designing the robust DP controllers, this task is accomplished by introducing appropriate frequency weighting functions and performance signals. The latter will be addressed in detail in the next section.

In extreme seas with high wave heights and/or long wave lengths or in swell dominated seas, the assumption of producing control action from the LF motion signals only, may not be so evident, as the WF motions (due to long wave lengths and thereby low frequency) will enter the control bandwidth of the DP system. Furthermore, in extreme

sea states limitation of power and loss of thrust due to ventilation, cavitation, and thruster-hull interactions will give reduced performance. See Sørensen (2002, 2011b) for details on DP in extreme sea condition. In extreme sea condition the wave filtering is turned off and all the components of motion are compensated in the DP controller to the extent that the propulsion system allows.

In the following sections, the design of a robust DP controller will be addressed separately for normal (calm to high) seas and extreme seas.

3. Control plant model DP vessels

In what follows, the vessel model, that is by now standard,[2] is presented. See Fossen and Strand (1999) and Sørensen (2011a). The model admits the realization

$$\dot{\xi}_W = A_W(\omega_0)\xi_W + E_W w_W \tag{1}$$

$$\eta_W = R(\psi_L)C_W\xi_W \tag{2}$$

$$\dot{b} = -T^{-1}b + E_b w_b \tag{3}$$

$$\dot{\eta}_L = R(\psi_L)\nu \tag{4}$$

$$M\dot{\nu} + D\nu = \tau + R^T(\psi_{tot})b \tag{5}$$

$$\eta_{tot} = \eta_L + \eta_W \tag{6}$$

$$\eta_y = \eta_{tot} + v \tag{7}$$

where (1) and (2) capture the 1st-order wave induced motion in surge, sway, and yaw; Eq. (3) represents the 1st-order Markov process approximating the unmodelled dynamics and the slowly varying bias forces (in surge and sway) and torques (in yaw) due to waves (2nd order wave induced loads), wind, and currents. The latter are given in earth fixed coordinates but expressed in body-axis. In the above, $\eta_W \in \mathbb{R}^3$ is the vessel's WF motion due to 1st-order wave-induced disturbances, consisting of WF position (x_W, y_W) and WF heading ψ_W of the vessel; $w_W \in \mathbb{R}^3$ and $w_b \in \mathbb{R}^3$ are zero mean Gaussian white noise vectors, and

$$A_W = \begin{bmatrix} 0_{3\times3} & I_{3\times3} \\ -\Omega_{3\times3} & -\Lambda_{3\times3} \end{bmatrix}, \quad E_W = \begin{bmatrix} 0_{3\times1} \\ I_{3\times1} \end{bmatrix}, C_W = [0_{3\times3}\ I_{3\times3}],$$

with

$$\Omega = \mathrm{diag}\{\omega_{01}^2, \omega_{02}^2, \omega_{03}^2\}, \Lambda = \mathrm{diag}\{2\zeta_1\omega_{01}, 2\zeta_2\omega_{02}, 2\zeta_3\omega_{03}\},$$

where ω_{0i} and ζ_i are the Dominant Wave Frequency (DWF) and relative damping ratio, respectively. Matrix $T = \mathrm{diag}(T_x, T_y, T_\psi)$ is a diagonal matrix of positive bias time constants and $E_b \in \mathbb{R}^{3\times3}$ is a diagonal scaling matrix. Vector $\eta_L \in \mathbb{R}^3$ consists of LF, earth-fixed position (x_L, y_L) and LF heading ψ_L of the vessel relative to an earth-fixed frame, $\nu \in \mathbb{R}^3$ represents the velocities decomposed into a vessel-fixed reference, and $R(\psi_L)$ is the standard orthonormal yaw angle rotation matrix (see Fossen, 2011 for details). Eq. (5) describes the vessels's LF motion at low speed (see Fossen, 2011), where $M \in \mathbb{R}^{3\times3}$ is the generalized system inertia matrix including zero-frequency added mass components, $D \in \mathbb{R}^{3\times3}$ is the linear damping matrix, and $\tau \in \mathbb{R}^3$ is a control vector of generalized forces generated by the propulsion system, that is, the main propellers aft of the ship and thrusters which can produce surge and sway forces as well as a yaw moment. Vector $\eta_{tot} \in \mathbb{R}^3$ describes the vessel's total motion, consisting of total position (x_{tot}, y_{tot}) and total heading ψ_{tot} of the vessel. Finally, (7) represents the position and heading measurement equation, with $v \in \mathbb{R}^3$ a zero-mean Gaussian white measurement noise.

Usually, in the design of controllers or observers for DP systems (especially for station keeping missions), the following assumptions are made. These assumptions are widely used in the literature, see Fossen and Strand (1999):

Assumption 1. The position and heading sensor noises are neglected, that is, v=0.[3]

Assumption 2. The amplitude of the wave-induced yaw motion ψ_W is assumed to be small, that is, less than 2–3° during normal operation of the vessel and less than 5° in extreme weather conditions. Hence, $R(\psi_L) \approx R(\psi_L + \psi_W)$. From Assumption 1 it follows that $R(\psi_L) \approx R(\psi_y)$, where $\psi_y \cong \psi_L + \psi_W$ denotes the measured heading.

Assumption 3. Low speed assumption, implying that the time-derivative of the total heading $\dot{\psi}_{tot}$ is bounded and close to zero.

We will also exploit the model property that the bias time constants in the x and y directions are equal, i.e. T_x=T_y.

In what follows we will consider a reference frame consisting of *vessel parallel coordinates* as introduced in Fossen (2011) and Sørensen (2011a). In sea keeping analysis (vessel motions in waves) the hydrodynamic frame is generally moving along the desired path of the vessel with the x-axis positive forwards to desired heading ψ_d, y-axis positive to the starboard, and z-axis positive downwards. The XY-plane (in hydrodynamic frame) is assumed to be fixed and parallel to the mean water surface. The vessel is assumed to oscillate with small amplitudes about this frame such that linear theory can be used to model perturbations. In station keeping operations (Dynamic Positioning) about desired coordinates x_d, y_d, and ψ_d, the hydrodynamic frame is Earth-fixed and denoted as the reference parallel frame. It is defined in a reference frame fixed to the vessel, with axes parallel to the earth-fixed frame and the origin is translated to the desired x_d and y_d (in this study we assume that $x_d = y_d = \psi_d = 0$).[4] Let $\eta_L^p \in \mathbb{R}^3$ denote the LF position (x_L^p, y_L^p) and LF heading $\psi^p{}_L$ of the vessel, respectively expressed in body coordinates, defined as

$$\eta_L^p = R^T(\psi_{tot})\eta_L. \tag{8}$$

Computing its derivative with respect to time yields

$$\dot{\eta}_L^p = \dot{R}^T(\psi_{tot})\eta_L + R^T(\psi_{tot})\dot{\eta}_L = \dot{R}^T(\psi_{tot})R(\psi_{tot})\eta_L^p + R^T(\psi_{tot})R(\psi_L)\nu \tag{9}$$

Using a Taylor series to expand $R^T(\psi_{tot})$ about ψ_L and neglecting higher order terms, it follows that

$$R^T(\psi_{tot})R(\psi_L) \cong I + \psi_W S, \tag{10}$$

where

$$S = \begin{bmatrix} 0 & 1 & 0 \\ -1 & 0 & 0 \\ 0 & 0 & 0 \end{bmatrix}.$$

Using simple algebra we obtain

$$\dot{R}^T(\psi_{tot})R(\psi_{tot}) = \dot{\psi}_{tot}S. \tag{11}$$

From (9) to (11) we conclude that

$$\dot{\eta}_L^p \approx \dot{\psi}_{tot}S\eta_L^p + \nu + \psi_W S\nu. \tag{12}$$

We now study the time evolution of the slowly varying bias forces, b, expressed in the vessel parallel coordinates, b^p, as follows:

$$b^p = R^T(\psi_{tot})b. \tag{13}$$

Clearly,

[2] The model described by (1)–(6) has minor differences with respect to the ones normally described in the literature. While in most of the references the WF components of motion are modelled in a fixed-earth frame, in this paper the WF motion is modelled in body-frame. The reader is referred to Hassani et al. (2012d,e) and Hassani and Pascoal (2015) for details and improvements of the present model.

[3] At this point, we stress that the noise free assumption is only used to derive a control plant model but later on, in the design process and simulation and verification, the effect of the measurement noise will be considered.

[4] Assuming $\psi_d = 0$, the reference parallel frame and vessel parallel frame coincide.

$$b = R(\psi_{tot})b^p, \tag{14}$$

and differentiating both sides yields

$$\dot{b} = \dot{R}(\psi_{tot})b^p + R(\psi_{tot})\dot{b}^p. \tag{15}$$

Using (3), (14) and (15) we obtain

$$\dot{R}(\psi_{tot})b^p + R(\psi_{tot})\dot{b}^p = -T^{-1}R(\psi_{tot})b^p + E_b w_b. \tag{16}$$

Reordering (16) and multiplying both sides by $R^T(\psi_{tot})$ gives

$$\dot{b}^p = -R^T(\psi_{tot})T^{-1}R(\psi_{tot})b^p - R^T(\psi_{tot})\dot{R}(\psi_{tot})b^p + R^T(\psi_{tot})E_b w_b. \tag{17}$$

Using the assumption that T_x=T_y, it can be checked that $R^T(\psi_{tot})T = TR^T(\psi_{tot})$; simple algebra also shows that $R^T(\psi_{tot})\dot{R}(\psi_{tot}) = -\dot{\psi}_{tot}S$.

Eq. (17) can be expressed as

$$\dot{b}^p = -T^{-1}b^p + \dot{\psi}_{tot}Sb^p + R^T(\psi_{tot})E_b w_b. \tag{18}$$

Summarizing the equations above yields

$$\dot{\xi}_W = A_W(\omega_0)\xi_W + E_W w_W \tag{19}$$

$$\eta_W = R(\psi_L)C_W\xi_W \tag{20}$$

$$\dot{b}^p = -T^{-1}b^p + \dot{\psi}_{tot}Sb^p + R^T(\psi_{tot})E_b w_b \tag{21}$$

$$\dot{\eta}_L^p = \dot{\psi}_{tot}S\eta_L^p + \nu + \psi_W S\nu \tag{22}$$

$$M\dot{\nu} + D\nu = \tau + b^p \tag{23}$$

Moreover, using Assumptions 1–3 a linear model with parametric uncertainty is obtained that is given by

$$\dot{\xi}_W = A_W(\theta_1)\xi_W + E_W w_W \tag{24}$$

$$\eta_W^b = C_W\xi_W \tag{25}$$

$$\dot{b}^p = -T^{-1}b^p + \theta_2 Sb^p + w_b^f \tag{26}$$

$$\dot{\eta}_L^p = \theta_2 S\eta_L^p + \nu + \theta_3 S\nu \tag{27}$$

$$M\dot{\nu} + D\nu = \tau + b^p \tag{28}$$

$$\eta_y^f = \eta_L^p + \eta_W^b + n \tag{29}$$

where η_W^b are WF components of motion on body-coordinate axis, and w_b^f and η_y^f are a new modified disturbance and a modified measurement defined by $w_b^f = R^T(\psi_y)E_b w_b$ and $\eta_y^f = R^T(\psi_y)\eta_y$, respectively,[5] $n \in \mathbb{R}^3$ is the measurement noise, and finally θ_1, θ_2, and θ_3 are ω_0, $\dot{\psi}_{tot}$, and ψ_W, respectively, which will be treated as parametric uncertainties.[6]

4. Robust DP controller design in normal sea conditions

This section describes the application of $\mathcal{H}_\infty$-based, μ synthesis controller design techniques to the solution of the DP problem. See Skogestad and Postlethwaite (2006) and Francis (1987) for an introduction to these techniques and Balas (2009) and Balas et al. (2016) for a mixed-μ design suite implemented in Matlab. In what follows, we adopt the general setup and nomenclature in the seminal work of Doyle et al. (1989). This leads to the standard feedback system of Fig. 1(a), where w is the input vector of exogenous signals, z is the output vector of errors and performance signals to be reduced, y is the vector of measurements that are available for feedback, and u is the vector of actuator signals. Suppose that the feedback system is well-posed, and let $T_{wz}(s)$ denote the closed loop transfer matrix from w to z. The $\mathcal{H}_\infty$, synthesis problem is to find, among all controllers that yield a stable closed loop system, a controller K that minimizes the infinity norm $\| T_{wz}(s) \|_\infty$ of $T_{wz}(s)$. We remind the reader that $\| T_{wz}(s) \|_\infty$ equals $\sup\{\sigma_{max}(T_{wz}(j\omega)): \omega \in \mathbb{R}\}$ where $\sigma_{max}(.)$ denotes the maximum singular value. Furthermore, $\| T_{wz} \|_\infty$ may be interpreted as the maximum energy gain of the closed loop operator T_{wz}. In mixed-μ synthesis, the structured singular value of a linear fractional transformation (LFT) of the plant and controller are used instead of the maximum singular values. The Structured Singular Values, denoted SSV or complex-μ (later modified to mixed-μ), were introduced in Doyle (1982) and Packard and Doyle (1993). In order to obtain a good design for a controller K, accurate knowledge of the plant is required. In practice, obtaining an accurate process model of the plant is almost impossible. The model may be inaccurate and there may be unmodelled dynamics and parametric uncertainties in the plant. To deal with this problem, the concept of model uncertainty must be considered. The unknown plant P is assumed to belong to a "legal" class of control plant models, $\mathcal{P}$, built around a nominal model P_0. The set of models $\mathcal{P}$ is characterized by a matrix Δ, which can be either a full matrix or a block diagonal matrix that includes all possible system structured uncertainties. We also use the weighting matrices (and incorporate them into P) to express the uncertainty in terms of normalized uncertainties in such a way that $\| \Delta(s) \|_\infty \leq 1$. The general control configuration in Fig. 1(a) may be extended to include model uncertainty as shown in Fig. 1(b).

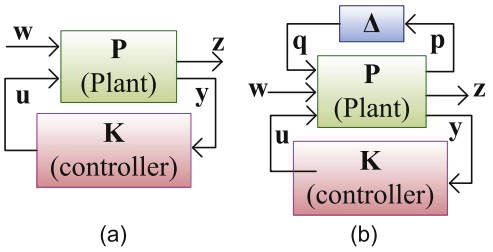

Fig. 1. Standard feedback configuration (with and without uncertainty).

Fig. 2 shows the nominal setup for designing a robust controller. Later, this setup will be used to form the standard feedback system of Fig. 1 which will be used in the mixed-μ synthesis methodology (Balas, 2009; Balas et al., 2016). To this effect, we design a robust DP controller which yields stability and performance robustness; using the mixed-μ software (see Balas, 2009; Balas et al., 2016), the performance parameter A_p in Fig. 2 is increased as much as possible, until the upper-bound on the mixed-μ, $\mu_{ub}(\omega)$, satisfies the inequality

$$\mu_{ub}(\omega) \leq 1 \quad \forall\, \omega. \tag{30}$$

In what follows we explain the different blocks of Fig. 2 in detail. Using the control model of the marine vessel given in (24)–(29), a state-space representation of the plant, including the disturbance and noise inputs, is given by

$$\dot{x}(t) = A(\theta)x(t) + B\,u(t) + L\,w(t),\ y(t) = C_1x(t) + v(t),\ z(t) = C_2x(t),$$

where $u(t) = \tau(t)$ is a control vector of generalized forces generated by the propulsion system, $w(t) = [w_W \;\; w_b^f]^T$ is a disturbance vector, $v(t)$ is the measurement noise, $y(t)$ is the measured output (total motion in body-frame), $z(t)$ is the performance signal (LF component of motion in parallel-frame), the state vector is $x(t) = [\xi_W^T \;\; \eta_L^{pT} \;\; \nu^T \;\; b^{pT}]^T$, and the system matrices $(A(\theta), B, C_1, C_2)$ are defined in the obvious manner. Notice that the $A(\theta)$ matrix contains parametric uncertainties (θ_1, θ_2, and θ_3) as defined before. We assume that the pairs $(A(\theta), B)$ and $(A(\theta), C_1)$ are controllable and observable, respectively, for all admissible parameter values.

Table 1 shows the definition of the sea conditions associated with the particular model of offshore supply vessel that is used in our study.

[5] When designing observers for wave filtering in DP, since the controller regulates the heading of the vessel, the designer can assign a new intensity to w_b^f; however, assigning the intensity of the noise in practice requires considerable expertise.

[6] In this paper, during the controller design process θ_1, θ_2 and θ_3 are treated as fixed parametric uncertainties. The methodology introduced can be extended to deal with time-varying parametric uncertainties with bounded rates of variation; see Rosa et al. (2009).

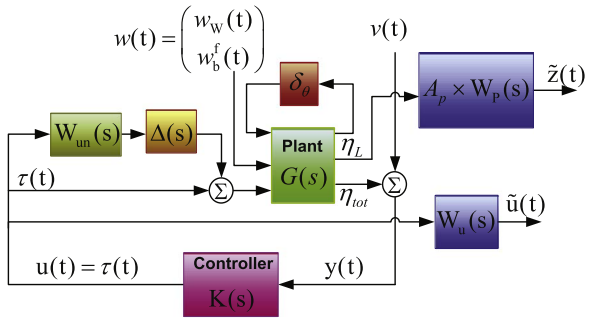

Fig. 2. Nominal setup with frequency weighting functions to design a robust controller.

Table 1
Definition of sea states.

Sea states	DWF ω_0 (rad)	Significant wave height H_s (m)
Calm seas	>1.11	<0.1
Moderate seas	[0.74 1.11]	[0.1 1.69]
High seas	[0.53 0.74]	[1.69 6.0]
Extreme seas	<0.53	>6.0

Table 2
Interval of parametric uncertainties.

Sea States	θ_1 (rad/s)	θ_2 (rad/s)	θ_3 (rad/s)
Calm seas	[1.11 1.8]	Int[a]	[−0.038 0.038]
Moderate seas	[0.74 1.11]	Int	[−0.04 0.04]
High seas	[0.53 0.74]	Int	[−0.042 0.042]
Extreme seas	[0.39 0.53]	Int	[−0.04 0.04]

[a] Int=[-5×10^{-4} 5×10^{-4}].

In the study we will design a robust DP controller for four different scenarios: calm seas, moderate seas, high seas, and extreme seas. The intervals of parametric uncertainty for θ in the four different scenarios are given in Table 2.[7]

4.1. Frequency weighting functions

As is well known, given a plant with structured and unstructured uncertainty it is not possible in general to obtain (by proper controller design) robust stability and performance uniformly, across all frequencies, where the latter is measured with the help of properly chosen performance signals. For this reason, it is crucial (for $\mathcal{H}_\infty$ control systems design) that frequency-dependent performance weights be introduced so as to reflect desired performance objectives over different frequencies. Appropriate selection of these weights provides flexibility in the control design process. The DP control design methodology that we propose builds heavily on the new design model introduced here and exploits the difference in the frequency contents of η_L and η_W. In the process, the choice of a weighting function for low frequency disturbance attenuation purposes is crucial.

During the process of robust DP controller design, we used the mixed-μ synthesis toolbox to maximize A_P (in Fig. 2) while making sure that robust stability and performance are observed. Fig. 3 depicts graphically the magnitude of the frequency response of the nominal performance weighting transfer function, $W_P(s)$. We remark that the performance weight $W_P(s)$ penalizes output $\eta^P{}_L$ in the low frequency range where the slowly varying disturbance b^P has most of its effect.

[7] The selection of parametric uncertainty interval for θ_1 seems natural (followed from Table 1). In order to select an uncertainty interval for θ_2 and θ_3 we have used a lengthy time simulation of the vessel and observed the variation of θ_2 and θ_3 during the simulation.

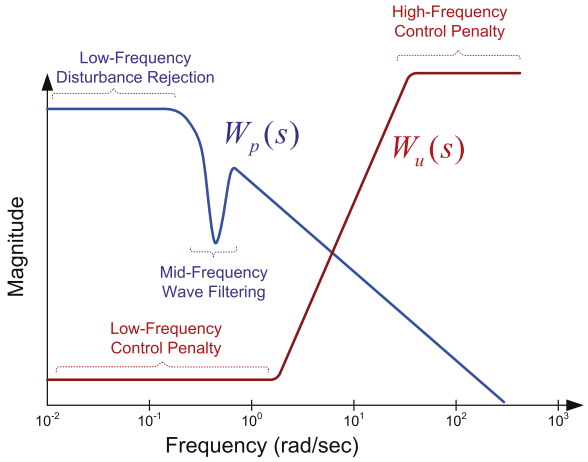

Fig. 3. Choice of weighting functions $W_P(s)$ and $W_u(s)$.

The gain parameter A_P in $W_P(s)$ specifies our desired level of LF disturbance-rejection. The larger the A_P, the greater the penalty on the effect of the disturbances on the LF motion. For superior disturbance-rejection in the LF range, A_P should be as large as possible. Moreover, the performance weight $W_P(s)$ places a smaller penalty on performance output $\eta^P{}_L$ in the mid-range frequencies where WF motion has most of its effect. In particular, this selection dictates our wave filtering demands to the $\mathcal{H}_\infty$ controller. Such a $W_P(s)$ can be found by cascading a low-pass and a narrow band-pass filter together, see Fossen (2011) and Sørensen (2011a) for details of DP wave filtering using cascaded low-pass and notch filtering. Wave filtering using KF or passivity based observer often gives a similar effect.

To reduce the thruster modulation to the lowest possible level, an appropriate weighting function should be chosen to penalize the control action differently over different frequencies. The rational is that the weight should be selected so that the control energy is penalized in the high-frequency. This avoids saturation as well as excitation of the high-frequency dynamics. The magnitude of the frequency response of a nominal control weighting transfer function, $W_u(s)$, is presented graphically in Fig. 3. This selection allows for larger control activity in lower frequencies and penalizes large controls at higher frequencies.

4.2. Unmodelled dynamic and unstructured uncertainty

Robust controllers designed using mixed-μ synthesis can yield robust stability and performance in the presence of both parametric uncertainty and unstructured uncertainties (or unmodelled dynamics). In the work of Katebi et al. (1997), a robust $\mathcal{H}_\infty$ controller is designed by minimizing the infinity norm of the transfer matrix from disturbances to a performance signal. That being done, the authors examined what amount of unmodelled dynamics could be tolerated in the feedback loop, using a small gain theorem. Clearly, such formulation may lead to conservative results. In this paper we aim for less conservative results with maximum performance and also simplicity in the design procedure. To capture the effect of unmodelled dynamics in our control plant model, it is also assumed that input forces and torque are provided through an actuator whose bandwidth is unknown but in some fixed known interval and its DC gain has 2 percent uncertainty; this amplifier can be described in the form of some nominal first order transfer function $G_0(s)$ and a multiplicative uncertainty described with some transfer function $W_{\text{unc}}(s)$. The computed frequency-domain upper-bound for the unstructured uncertainty, which serves in this example as a surrogate for unmodelled dynamics, $W_{\text{unc}}(s)$, captures some important practical features. This implies that the designed controller $K(s)$ provides robust-stability and performance for the nominal vessel model with some percentage of

model perturbation (one can easily compute its exact value) over different frequencies. Later in Section 6 we show in detail how an specific selection of $W_{\text{unc}}(s)$ specifies the percentage of model perturbation, that can be dealt by robust controller, over different frequencies.

Summarizing our design process, Fig. 4 shows the appropriate augmented structure for DP $\mathcal{H}_\infty$ controller design.

5. Robust DP controller design in extreme sea condition

In extreme seas and extreme conditions the nonlinearities due to large motions will be more noticeable for the WF motions. Also, the coupling between the horizontal plane motions and the vertical motions will become more important. As the sea state builds, it is also a challenge to distinguish the LF motions from the WF motions. At higher sea states, the period of the waves gets longer, resulting in decreasing wave frequencies. Thus, the formulation of hydrodynamics models appropriate for controller designs is still a subject for research. In such conditions (extreme seas or swell with very long wave periods) wave filtering should be turned off, see Sørensen (2011b), and in particular Sørensen et al., 2002 for details on the effect of wave filtering in extreme seas. Based on Sørensen et al. (2002) the state space control plant model for DP in extreme sea can be described by

$$\dot{b} = -T^{-1}b + E_b w_b \tag{31}$$

$$\dot{\eta} = R(\psi)\nu \tag{32}$$

$$M\dot{\nu} + D\nu = \tau + R^T(\psi)b \tag{33}$$

$$\eta_y = \eta + v \tag{34}$$

which is similar to the one in (1)–(7), excluding the WF motion components. To design a robust DP controller for extreme sea conditions, the methodology explained in the previous section can be used. However, the performance signal will be the total motion (and not only LF part of it) and the frequency weighting functions must be changed. We suggest a new frequency weighting function $W_P(s)$ as

$$W_p(s) = A_p W_L(s)$$

where $W_L(s)$ is some low-pass filter and $W_P(s)$ is applied to the total motion of the vessel, i.e. the controller should compensate for both LF and WF motions.

6. Controller design summary

In this section we study the process of designing the robust controllers for a specific marine vessel. For operating conditions from calm to high seas, the transfer function of the performance weight upon the output η_L^p is selected as

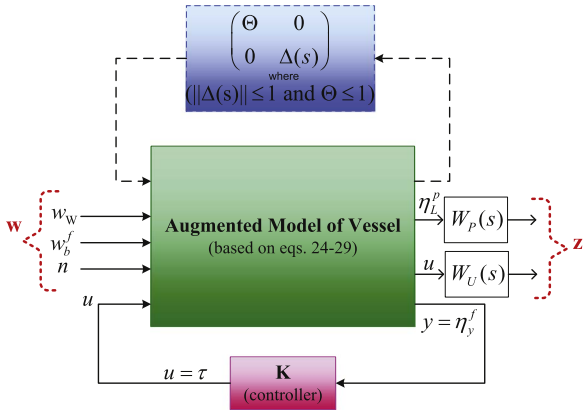

Fig. 4. Standard feedback configuration developed for DP.

Table 3
Weighting functions' coefficients.

Calm	α	[0.0008 1.3498 0.3955 2.8633]
	β	[1.000 4.4722 6.2482 2.8633]
Moderate	α	[0.0059 0.8612 0.1689 0.7543]
	β	[1.0000 3.0957 2.6665 0.7543]
High	α	[0.0060 0.6080 0.0823 0.2521]
	β	[1.0000 2.1406 1.2811 0.2521]

$$W_p(s) = A_p \frac{\alpha_1 s^3 + \alpha_2 s^2 + \alpha_3 s + \alpha_4}{\beta_1 s^3 + \beta_2 s^2 + \beta_3 s + \beta_4} \tag{35}$$

where the coefficients of $\alpha = [\alpha_1\ \alpha_2\ \alpha_3\ \alpha_4]$ and $\beta = [\beta_1\ \beta_2\ \beta_3\ \beta_4]$, obtained after several iterations, are condensed in Table 3. The selection of the $W_P(s)$ for different sea conditions is done by cascading a low-pass and a notch filter together. The low-pass part is responsible for good low frequency disturbance rejection and the band pass filter (in mid range frequency) is tuned to have a bandwidth similar to the range of the frequencies that waves have their most (first order) effect on the motion (WF components of motion). Fig. 5 depicts the magnitude of the frequency response of the computed performance weighting transfer functions for A_P=1. In extreme sea conditions we suggest a new frequency weighting function $W_P(s)$ as

$$W_p(s) = A_p \frac{0.5}{s + 0.5} \tag{36}$$

which is applied to the total motion of the vessel, i.e. the controller should compensate for both LF and WF motions.

In this paper the control action is penalized with the frequency domain weight

$$W_u(s) = \frac{s^2 + 0.3652s + 0.0333}{s^2 + 36.52s + 333.43}.$$

Fig. 6 depicts the magnitude of the frequency response of the computed control action weighting transfer function. This selection allows for larger control action at lower frequencies and penalizes large control activity at higher frequencies. Throughout this paper the same weight is applied to all control channels.

We assume that input forces and torque applied to the vessel are provided through a first-order low pass actuator whose bandwidth is unknown but lies in the interval [2.46 4.10] rad/s; its DC gain has 2 percent uncertainty; this actuator can be described in the form of a nominal model $G_0(s)$ and multiplicative uncertainty $W_{\text{unc}}(s)$ as follows:

$$G_0(s) = \frac{1}{3.2859s + 1},\ W_{\text{unc}}(s) = \frac{2.9153s^2 + 0.9529S + 0.0200}{8.0978s^2 + 5.7503s + 1.0000}.$$

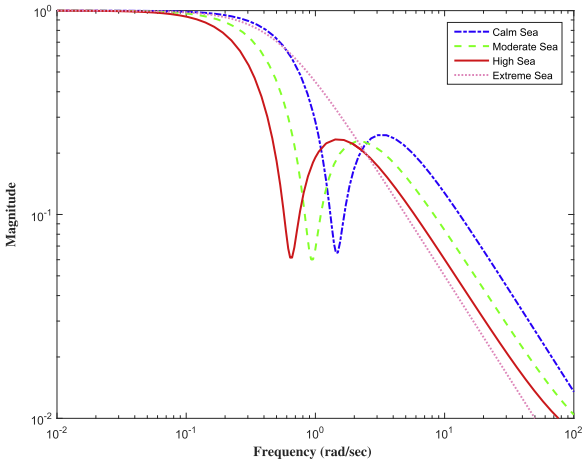

Fig. 5. Choice of weighting functions $W_P(s)$ for A_P=1.

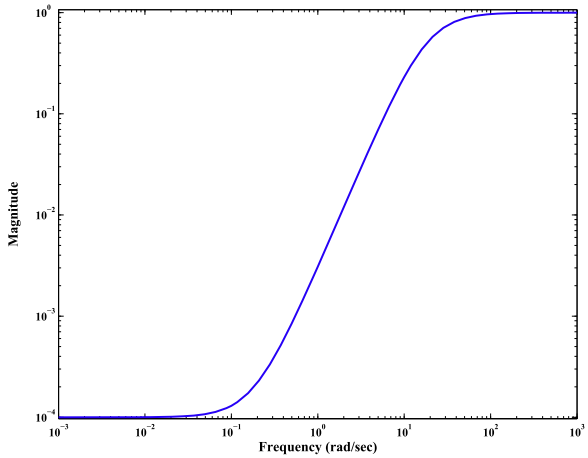

Fig. 6. Choice of weighting functions $W_u(s)$ to penalize the control action.

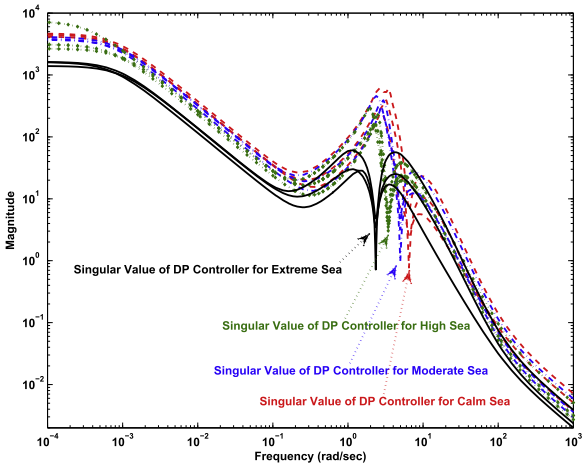

Fig. 7. Singular values of the local $\mathcal{H}_\infty$ DP controllers for calm to extreme seas.

The computed frequency-domain upper-bound for the unstructured uncertainty, which serves in this example as a surrogate for unmodelled dynamics, $W_{\text{unc}}(s)$, captures some important practical features. This implies that the designed controller $K(s)$ provides robust-stability and performance for the nominal vessel model with 9–33% model perturbation (in each control channel, independently) over the frequency range from 0.1 to 1 rad/s, and almost 35% model perturbation, for frequencies over 1 rad/s. Recalling the frequency content of the disturbances in the DP applications, one can verify how a particular selection of $W_{\text{unc}}(s)$ can capture the effect of different disturbances over the dynamics of the vessel.

Table 4 summarizes the results of the design of robust DP controllers for different sea conditions. As expected, the best performance index, i.e. A_P, is achieved for calm sea condition and the worst is for extreme sea.

Note that all controllers are three-input three-output LTI systems since the controllers produce surge and sway forces as well as a yaw moment, and measurements are available for three states: surge, sway and heading. Fig. 7 compares the four local controllers by examining their singular value plots; it is clear that at low frequencies the local controllers generate a larger gain and in mid-range frequencies (where WF motion has its maximum effect) the local controllers generate a (significantly) lower gain; naturally, this leads to good disturbance-rejection in low frequencies and wave filtering in mid-range frequencies. We emphasize that each individual local controller has guaranteed performance- and stability-robustness over its associated parameter subintervals of Table 2. Due to the fact that the mixed-μ upper-bound inequality of $\mu \leq 1$ is only a sufficient condition for both robust-stability and robust-performance, each local controller will actually have a wider stability region, see Vasconcelos et al. (2009).

Fig. 8 illustrates the potential wave filtering effect of the robust DP controllers in calm to extreme sea conditions by using plots of the maximum singular value of the closed loop system from control channel (where the effect of the waves enters as forces in surge and sway and torques in yaw) to the output position of the vessel. For calm to high sea conditions, it is shown that a band-pass kind of effect exists such that the mid-range frequency components of the vessel's motion are not counterbalanced by controller where such effect is not seen in extreme sea condition and the WF components of motion are also regulated by the robust controller (in extreme sea).

Table 4
Summary of controller performance index.

Controller	A_P	μ
Calm sea	3	$0.99 \leq \mu < 1$
Moderate sea	2.5	$0.99 \leq \mu < 1$
High sea	1.9	$0.99 \leq \mu < 1$
Extreme sea	1	$0.99 \leq \mu < 1$

7. Numerical simulations

7.1. Overview of the simulator

In what follows we test the performance of our controllers using the Marine Cybernetics Simulator (MCSim), later on upgraded to Marine System Simulator (MSS). The MCSim is a modular multi-disciplinary simulator based on Matlab/Simulink. It was developed at the Department of Marine Technology, Norwegian University of Science and Technology (NTNU). The MCSim incorporates high fidelity models, denoted as process plant model or simulation model in Sørensen (2011a), at all levels (plants and actuators). It captures hydrodynamic effects, generalized Coriolis and centripetal forces, nonlinear damping and current forces, and generalized restoring forces. It is composed of different modules that include the following:

(1) *Environmental module*, containing different wave models, surface current models, and wind models.

(2) *Vessel dynamics module*, consisting of a LF and a WF model. The LF model is based on the standard 6 DOF vessel dynamics, whose inputs are the environmental loads and the interaction forces from thrusters and the external connected systems.

(3) *Thruster and shaft module*, containing thrust allocation routine for non-rotating thrusters, thruster dynamics and local thruster control. It may also include advanced thrust loss models for extreme seas, in which case detailed information about waves, current and vessel

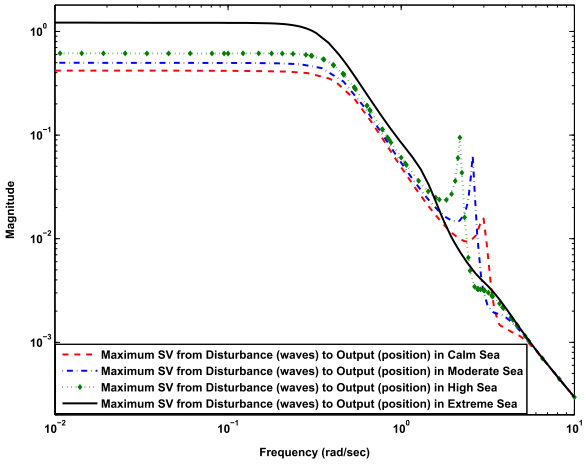

Fig. 8. Maximum singular value of the closed-loop system for calm to extreme seas.

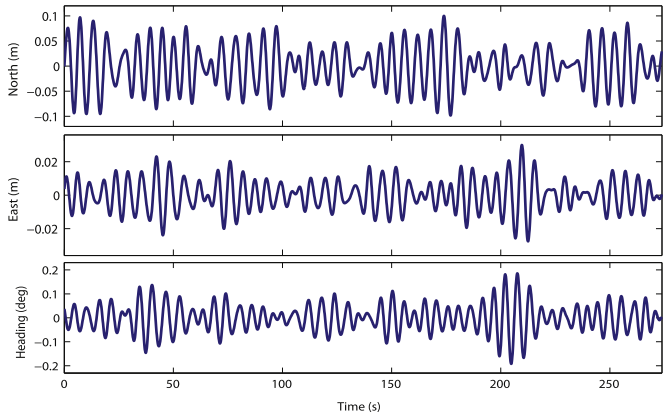

Fig. 9. Simulation results: total position and heading of the DP system using robust DP controller in calm sea condition.

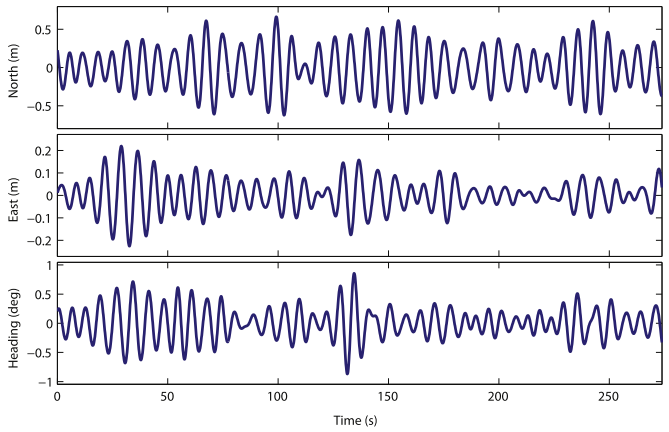

Fig. 10. Simulation results: total position and heading of the DP system using robust DP controller in moderate sea condition.

motion is required. The shaft is modelled as a rotational mass, with propeller speed given from motor torque and propeller load torque.

(4) *Vessel control module*, consisting of different controllers, namely, nonlinear multivariable PID controller and Linear Quadratic Gaussian (LQG) controller, for DP. For more details on the MCSim see Sørensen et al. (2003), Perez et al. (2005, 2006), and Fossen and Perez (2009b).

7.2. Numerical simulations

This section described the results of simulations with the MCSim using the controllers designed in the previous sections.

Figs. 9–16 show the results of Monte-Carlo simulations of the robust DP system in different sea conditions.[8] From Figs. 13–16 it is seen also that even with using wave filtering frequency weighting functions (in the design process of the controllers), some of the 1st-order wave frequency components are seen in the LF components of motion.[9] Here we should highlight that in Figs. 13–16 we present only the LF components of the motion. However, the controllers are fed with the total position (LF+WF).

[8] All the results are presented in full scale. Moreover, we should highlight that the starting time of the simulation in Figs. 9–16 (and also Figs. 18–22) are different but have been transformed to zero for the sake of clarity.

[9] At this point, we should emphasize that the controllers are designed according to the simple model of (24)–(29), while they are tested in the MCSim with a high fidelity model that captures hydrodynamic effects, generalized Coriolis and centripetal forces, nonlinear damping and current forces, and generalized restoring forces. Moreover, in the MCSim the JONSWAP wave spectrum is used to simulate the waves while the linear model captures the wave effects with second order approximation of the waves' spectral density.

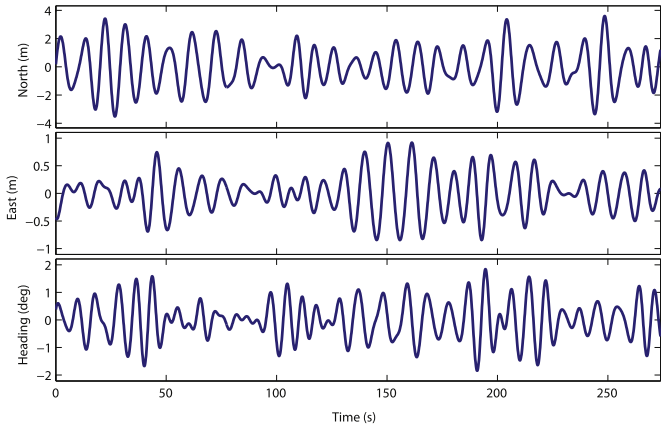

Fig. 11. Simulation results: total position and heading of the DP system using robust DP controller in high sea condition.

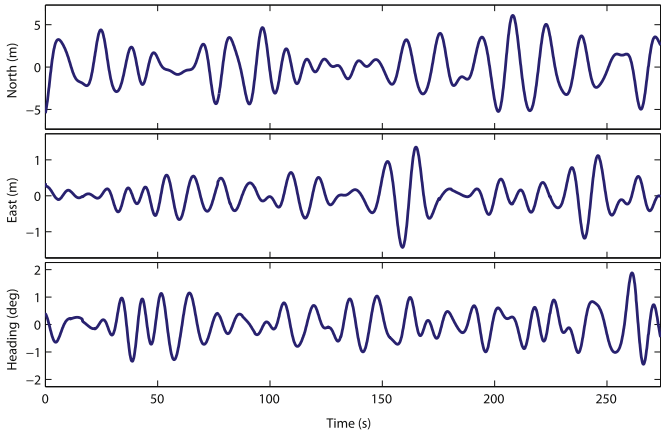

Fig. 12. Simulation results: total position and heading of the DP system using robust DP controller in extreme sea condition.

In these simulations, the different environment conditions from calm to high seas are simulated using the spectrum of the Joint North Sea Wave Project (JONSWAP), see Hasselmann et al. (1973). The calm, moderate, high and extreme seas are simulated with Dominant Wave Frequency (DWF) of 1.20 rad/s, 0.91 rad/s, 0.65 rad/s and 0.4 rad/s, respectively.

8. Experimental model test results

The designed controllers were tested using the model vessel, CybershipIII, at the Marine Cybernetic Laboratory (MCLab) of the Department of Marine Technology, Norwegian University of Science and Technology (NTNU). This section presents the experimental results of model tests for robust DP systems in different sea conditions produced by a hydraulic wave maker.

8.1. Overview of the CybershipIII

CyberShipIII is a 1:30 scaled model of an offshore vessel operating in the North Sea. Fig. 17 shows the vessel at the basin in the MCLab and Table 5 presents the main parameters of both the model and the full scale vessel.

CybershipIII is equipped with two pods located at the aft. A tunnel thruster and an azimuth thruster are installed in the bow.[10] It has a mass of m=75 kg, length of L=2.27 m and breadth of B=0.4 m. The internal hardware architecture is controlled by an onboard computer

[10] For technical reasons in this experiment the tunnel thruster was deactivated.

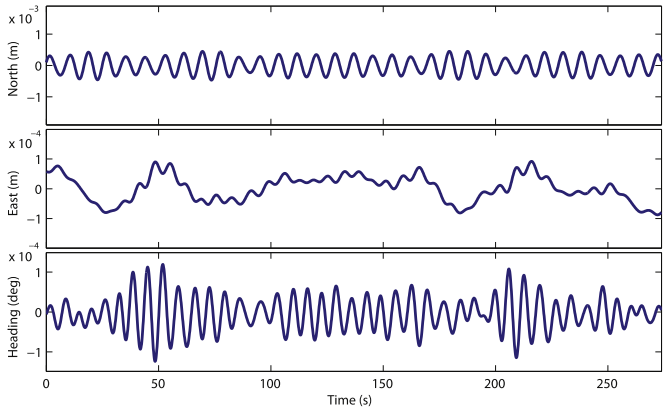

Fig. 13. Simulation results: LF position and heading of the DP system using robust DP controller in calm sea condition.

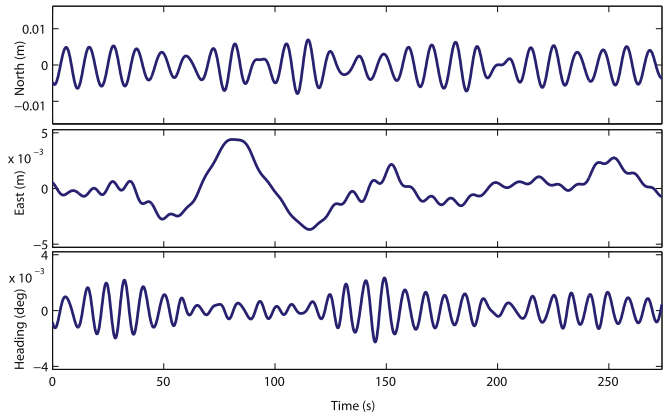

Fig. 14. Simulation results: LF position and heading of the DP system using robust DP controller in moderate sea condition.

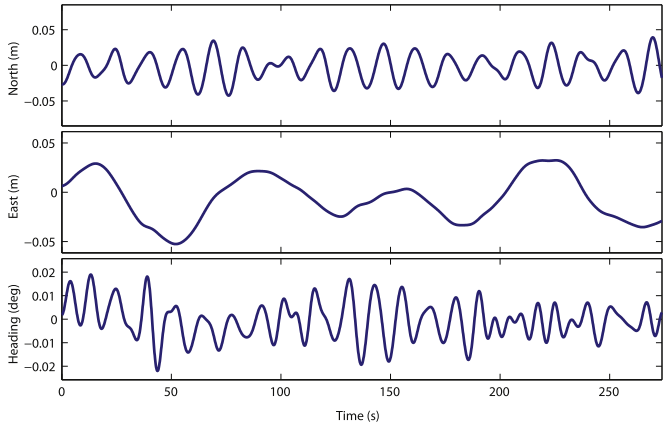

Fig. 15. Simulation results: LF position and heading of the DP system using robust DP controller in high sea condition.

that communicates with the onshore PC through a WLAN. The PC onboard the ship uses QNX real-time operating system (target PC). The control system is developed on a PC in the control room (host PC) under Simulink/Opal and downloaded to the target PC using automatic C-code generation and wireless Ethernet. The motion capture unit (MCU), installed in the MCLab, provides Earth-fixed position and heading of the vessel. The MCU consists of onshore 3-cameras mounted on the towing carriage and a marker mounted on the vessel. The cameras emit infrared light and receive the light reflected from the

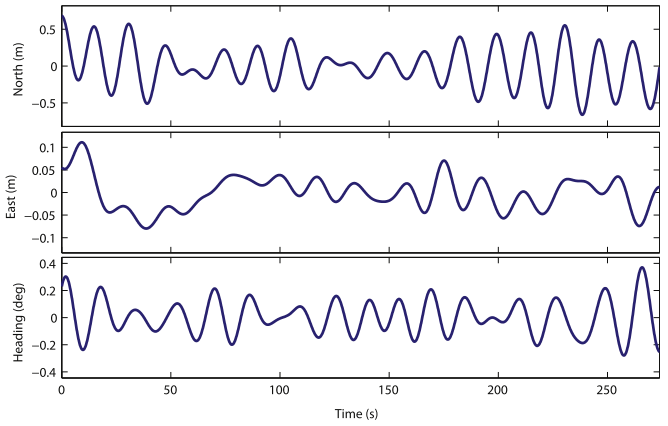

Fig. 16. Simulation results: LF position and heading of the DP system using robust DP controller in extreme sea condition.

Fig. 17. CybershipIII.

marker.

Table 5
Model main parameters.

Property	Model	Full scale
Overall length	2.275 m	68.28 m
Length between perpendiculars	1.971 m	59.13 m
Breadth	0.437 m	13.11 m
Breadth at water line	0.437 m	13.11 m
Draught	0.153 m	4.59 m
Draught front perpendicular	0.153 m	4.59 m
Draught aft. perpendicular	0.153 m	4.59 m
Depth to main deck	0.203 m	6.10 m
Weight (hull)	17.5 kg	Unknown
Weight (normal load)	74,2 kg	22.62 tons
Longitudinal center of gravity	100 cm	30 m
Vertical center of gravity	19.56 cm	5.87 m
Propulsion motors max shaft power (6% gear loss)	81 W	3200 HP
Tunnel thruster max shaft power (6% gear loss)	27 W	550 HP
Maximum speed	Unknown	11 knots

To simulate the different sea conditions a wave maker system, produced by the Danish Hydraulic Institute (DHI), is used. It consists of a single flap covering the whole Breadth of the basin, and a computer controlled motor, moving the flap. It is able to produce regular and irregular waves with different spectrums. We have used JONSWAP spectral for simulating the different sea conditions for our experiment.

8.2. Experimental results

Figs. 18–21 shows the vessel position and heading in different sea conditions. The results of the model test are in agreement with the ones obtain in the numerical simulation study, showing satisfactory performance of the robust DP controllers in different sea conditions.

The results of the experimental test are consistent with those obtained using the MCSim in the simulation study. The performance

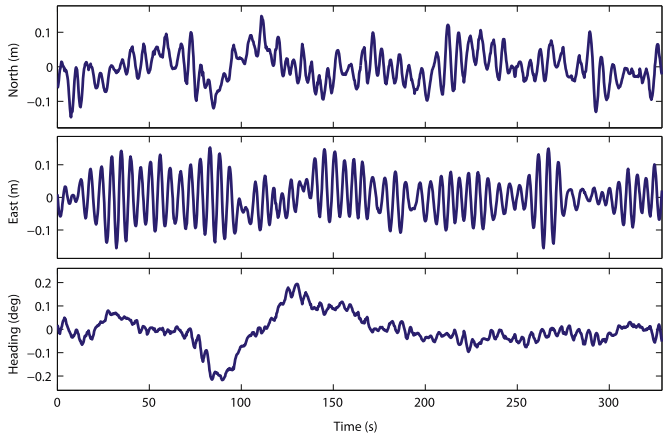

Fig. 18. Experimental results: total position and heading of the CybershipIII in DP operation using robust DP controller in calm sea condition.

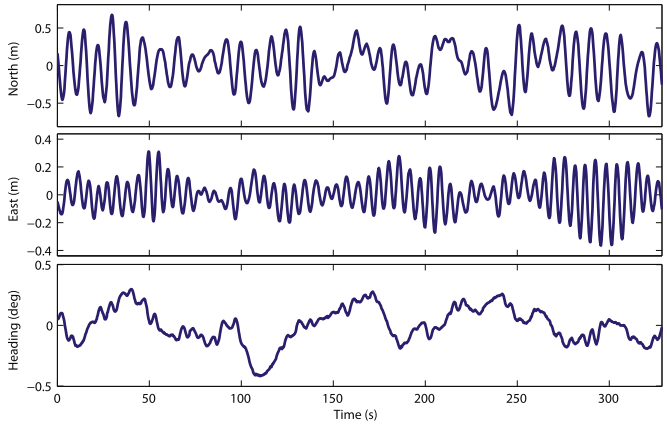

Fig. 19. Experimental results: total position and heading of the CybershipIII in DP operation using robust DP controller in moderate sea condition.

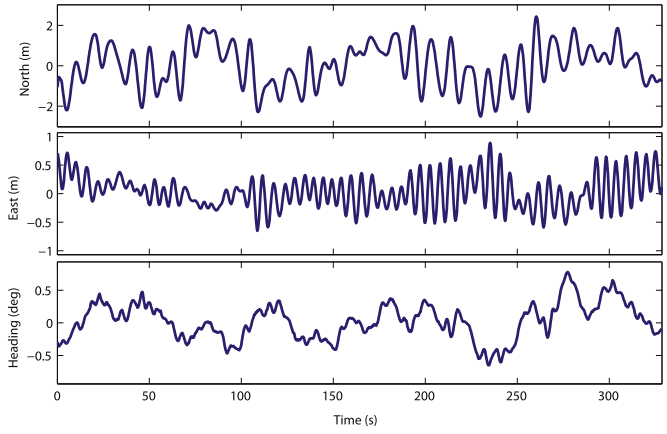

Fig. 20. Experimental results: total position and heading of the CybershipIII in DP operation using robust DP controller in high sea condition.

of the robust DP controllers designed for different sea conditions is compared with that obtained with LQG and PID controllers in Hassani et al. (2012a), Hassani and Pascoal (2015), both through numerical simulations using MCSim, and experimentally, using model test experiments. The results in Hassani et al. (2012a) and Hassani and Pascoal (2015) show satisfactory performance of robust DP controllers in different sea conditions; in particular, superior performance of robust DP controllers in extreme sea condition is shown in Hassani

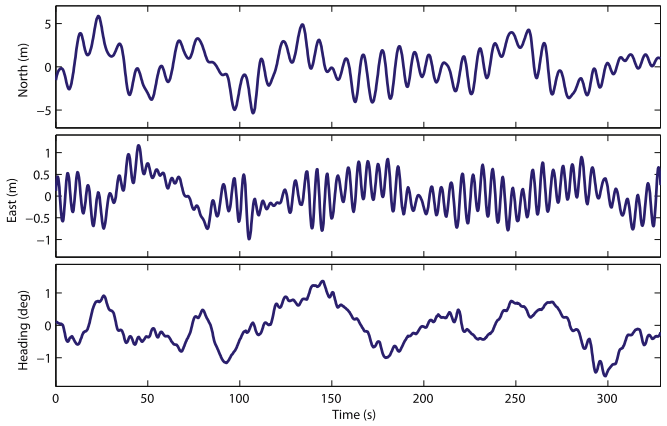

Fig. 21. Experimental results: total position and heading of the CybershipIII in DP operation using robust DP controller in extreme sea condition.

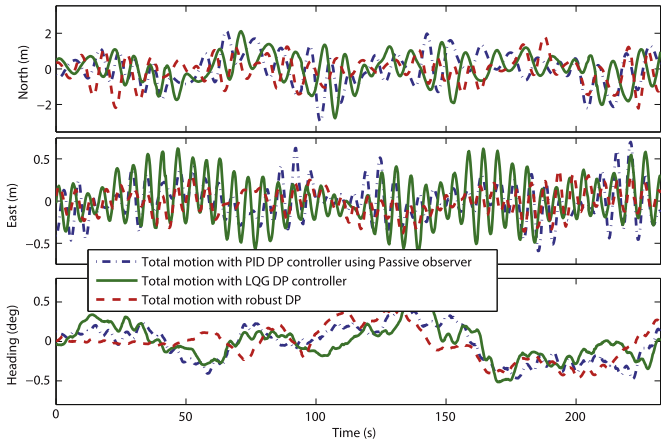

Fig. 22. Experimental results (high sea): total motion of the vessel with different DP controllers.

et al. (2012a) and Hassani and Pascoal (2015). Fig. 22 shows the comparison of the total motion of the vessel in high sea, working under different DP systems[11]; it is seen that the robust DP controller has a better performance in regulation of the vessel and two other controllers have similar performance. Table 6 shows the mean covariance of three station keeping experiments under the above-mentioned controllers. The table reveals better performance of the robust DP controller in the station keeping scenario when compared with the other two controllers.[12]

At this point we should also stress that the robust DP controllers designed using mixed-μ are usually of very high order. In this study the designed robust controllers were of order 120. We used model reduction and checked if the reduced order controllers still satisfied the closed-loop robust stability and performance requirements. The reduced order controllers have orders of (approximately) 30 in all cases and all of them satisfy robust performance and stability requirement introduced by μ synthesis methodology, and through the experiment

[11] The time index of the total motion of the vessel with different DP systems in Fig. 22 are different and figure serves only as a graphical qualitative comparison. For quantitative comparison see Table 6.

[12] We experienced around 20 percent performance improvement in high seas and around 30 percent performance in extreme seas. We should also stress that the performance degradation in heading is below the sensors accuracy and hereby does not provide useful information.

Table 6
Experimental results (high sea): calculated covariance of total motion of the vessel (average of three experiments).

Controller	x (m^2)	y (m^2)	ψ (deg^2)
PID with a passive observer	0.80	0.03	0.05
LQG controller	0.74	0.07	0.04
robust controller	0.62	0.02	0.09

they were discretized with a sampling time $T_s = 0.3$ s.

9. Conclusions

This paper proposed a new strategy for the design of robust DP controllers for marine vessels under different sea conditions using mixed-μ synthesis. A linear model of the vessel with parametric and unstructured uncertainties was developed and robust DP controllers were designed using mixed-μ synthesis. During the design process, a systematic and infinitive methodology was proposed to appropriately select the frequency weighting functions. We also offered a comprehensive evaluation of the performance obtained with a set of robust DP controllers designed for different sea conditions, for a representative vessel model. The evaluation included Monte-Carlo simulations, as well as model-test experiments with a vessel in a water tank equipped with a wave maker. The results obtained confirmed the efficacy of the methodology adopted for robust controller design. Future work will include the application of the methodology developed to the design of DP controllers for a real vessel.

Acknowledgement

We thank our colleagues A. Pedro Aguiar, N.T. Dong and Thor I. Fossen for many discussions on wave filtering and adaptive estimation. We would also like to thank T. Wahl, Øyvind Smogeli, M. Etemaddar, E. Peymani, M. Jalali, M. Shapouri, and B. Ommani for their great assistance during the model tests at MCLab.

References

Balas, G., Chiang, R., Packard, A., Safonov, M., 2016. Robust Control Toolbox: User's Guide (R2016a). Mathworks.
Balas, G.J., 2009. Mixed-μ software (unpublished version). Private communication.
Balchen, J., Jenssen, N.A., Sælid, S., 1976. Dynamic positioning using Kalman filtering and optimal control theory. In: The IFAC/IFIP Symposium on Automation in Offshore Oil Field Operation, Bergen, Norway, pp. 183–186.
Balchen, J., Jenssen, N.A., Sælid, S., 1980. A dynamic positioning system based on Kalman filtering and optimal control. Model. Identif. Control 1, 135–163.
Donha, D., Katebi, M.R., Grimble, M.J., 1997. Nonlinear ship positioning system design using an $\mathcal{H}_\infty$ controller. In: Proceedings of ECC'97 – European Control Conference, Brussels, Belgium.
Donha, D.C., Katebi, M.R., 2007. Automatic weight selection for controller synthesis. Int. J. Syst. Sci. 38, 651–664.
Doyle, J., 1982. Analysis of feedback systems with structured uncertainties. IEE Proc. Control Theory Appl. 129, 242–250.
Doyle, J.C., 1978. Guaranteed margins for LQG regulators. IEEE Trans. Autom. Control 23, 756–757.
Doyle, J.C., Glover, K., Khargonekar, P.P., Francis, B.A., 1989. State-space solutions to standard $\mathcal{H}_2$ and $\mathcal{H}_\infty$ control problems. IEEE Trans. Autom. Control 34, 831–847.
Faltinsen, O.M., 1990. Sea Loads on Ships and Offshore Structures. Cambridge University Press, UK.
Fossen, T.I., 2000. Nonlinear passive control and observer design for ships. Model. Identif. Control 21, 129–184.
Fossen, T.I., 2011. Handbook of Marine Craft Hydrodynamics and Motion Control. John Wiley & Sons. Ltd, Chichester, UK.
Fossen, T.I., Perez, T., 2009a. Kalman filtering for positioning and heading control of ships and offshore rigs. IEEE Control Syst. Mag. 29, 32–46.
Fossen, T.I., Perez, T., 2009b. Marine systems simulator (MSS). ⟨http://www.marinecontrol.org⟩.
Fossen, T.I., Sagatun, S.I., Sørensen, A.J., 1996. Identification of dynamically positioned ships. J. Control Eng. Pract. 4, 369–376.
Fossen, T.I., Strand, J.P., 1999. Passive nonlinear observer design for ships using Lyapunov methods: full-scale experiments with a supply vessel. Automatica 35, 3–16.
Francis, B., 1987. A Course in $\mathcal{H}_\infty$ Control Theory. Springer-Verlag, Berlin; New York.
Fung, P.T.K., Grimble, M.J., 1983. Dynamic ship positioning using self-tuning Kalman filter. IEEE Trans. Autom. Control 28, 339–349.
Grimble, M.J., Patton, R.J., Wise, D.A., 1980a. The design of dynamic ship positioning control systems using stochastic optimal control theory. Optim. Control Appl. Methods 1, 167–202.
Grimble, M.J., Patton, R.J., Wise, D.A., 1980b. The design of dynamic ship positioning control systems using stochastic optimal control theory. IEE Proc. 127, 93–102.
Hassani, V., Pascoal, A., 2015. Wave filtering and dynamic positioning of marine vessels using a linear design model: Theory and experiments. In: Ocampo-Martinez, C., Negenborn, R.R. (Eds.), Transport of Water versus Transport over Water. Operations Research/Computer Science Interfaces Series, vol. 58. Springer International Publishing Switzerland , pp. 315–343.
Hassani, V., Pascoal, A.M., Sørensen, A.J., 2013a. A novel methodology for adaptive wave filtering of marine vessels: theory and experiments. In: Proceedings of the 52nd IEEE Conference on Decision and Control. Firenze, Italy, pp. 6162–6167.
Hassani, V., Sørensen, A.J., Pascoal, A.M., 2012a. Evaluation of three dynamic ship positioning controllers: from calm to extreme conditions. In: Proceedings of NGCUV'12 – IFAC Workshop on Navigation, Guidance and Control of Underwater Vehicles, Porto, Portugal.
Hassani, V., Sørensen, A.J., Pascoal, A.M., 2012b. Robust dynamic positioning of offshore vessels using mixed-μ synthesis, Part I: designing process. In: Proceedings of ACOOG'12 – IFAC Workshop on Automatic Control in Offshore Oil and Gas Production, Trondheim, Norway, pp. 177–182.
Hassani, V., Sørensen, A.J., Pascoal, A.M., 2012c. Robust dynamic positioning of offshore vessels using mixed-μ synthesis, Part II: simulation and experimental results. In: Proceedings of ACOOG'12 – IFAC Workshop on Automatic Control in Offshore Oil and Gas Production, Trondheim, Norway, pp. 183–188.
Hassani, V., Sørensen, A.J., Pascoal, A.M., 2013b. Adaptive wave filtering for dynamic positioning of marine vessels using maximum likelihood identification: theory and experiments. In: Proceedings of the 9th IFAC Conference on Control Applications in Marine Systems. Elsevier, pp. 203–208.
Hassani, V., Sørensen, A.J., Pascoal, A.M., 2013c. A novel methodology for robust dynamic positioning of marine vessels: theory and experiments. In: Proceedings of the 2013 American Control Conference. IEEE. pp. 560–565.
Hassani, V., Sørensen, A.J., Pascoal, A.M., Aguiar, A.P., 2012d. Developing a linear model for wave filtering and dynamic positioning. In: Proceedings of CONTROLO'12 – The 10th Portuguese Conference on Automatic Control, Madeira, Portugal, pp. 298–303.
Hassani, V., Sørensen, A.J., Pascoal, A.M., Aguiar, A.P., 2012e. Multiple model adaptive wave filtering for dynamic positioning of marine vessels. In: Proceedings of ACC'12 – American Control Conference, Montreal, Canada, pp. 6222–6228.
Hasselmann, K., Barnett, T.P., Bouws, E., Carlson, H., Cartwright, D., Enke, K., Ewing, J.A., Gienapp, H., Hasselmann, D.E., Kruseman, P., Meerburg, A., Müller, P., Olbers, D.J., Richter, K., Sell, W., Walden, H., 1973. Measurements of wind-wave growth and swell decay during the joint north sea wave project (JONSWAP). Ergnzungsheft Dtsch. Hydrogr. Z. Reihe 8, 1–95.
Katebi, M.R., Grimble, M.J., Zhang, Y., 1997. $\mathcal{H}_\infty$ robust control design for dynamic ship positioning. IEE Proc. Control Theory Appl. 144, 110–120.
Katebi, M.R., Yamamoto, I., Matsuura, M., Grimble, M.J., Hirayama, H., Okamoto, N., 2001. Robust dynamic ship positioning control system design and application. Int. J. Robust Nonlinear Control 11, 1257–1284.
Martin, P., Katebi, M.R., Grimble, M.J., Yamamoto, I., 2000. Robust dynamic ship positioning. In: Proceedings of the 5th IFAC Conference on Manoeuvring and Control of Marine Craft (MCMC00), Aalborg, Denmark.
Packard, A., Doyle, J., 1993. The complex structured singular value. Automatica 29, 71–109.
Perez, T., Smogeli, O.N., Fossen, T.I., Sørensen, A.J., 2005. An overview of marine systems simulator (MSS): a simulink toolbox for marine control systems. In: Proceedings of Scandinavian Conference on Simulation and Modeling (SIMS'05), Trondheim, Norway.
Perez, T., Sørensen, A.J., Blanke, M., 2006. Marine vessel models in changing operational conditions—a tutorial. In: 14th IFAC Symposium on System Identification (SYSID'06), Newcastle, Australia.
Rosa, P., Balas, G., Silvestre, C., Athans, M., 2009. On the synthesis of robust multiple-model adaptive controllers (RMMAC) using BMI/LPV controllers. In: Proceedings of the 10th European Control Conference (ECC09), Budapest, Hungary.
Sælid, S., Jenssen, N.A., Balchen, J., 1983. Design and analysis of a dynamic positioning system based on Kalman filtering and optimal control. IEEE Trans. Autom. Control 28, 331–339.
Skogestad, S., Postlethwaite, I., 2006. Multivariable Feedback Control: Analysis and Design 2nd edition. Wiley, New York.
Sørensen, A.J., 2005. Structural issues in the design and operation of marine control systems. Annu. Rev. Control 29, 125–149.
Sørensen, A.J., 2011a. Lecture notes on marine control systems. Technical Report UK-11-76. Norwegian University of Science and Technology.
Sørensen, A.J., 2011b. A survey of dynamic positioning control systems. Annu. Rev. Control 35, 123–136.
Sørensen, A.J., Pedersen, E., Smogeli, O., 2003. Simulation-based design and testing of dynamically positioned marine vessels. In: Proceedings of the International Conference on Marine Simulation and Ship Maneuverability (MARSIM'03), Kanazawa, Japan.
Sørensen, A.J., Sagatun, S.I., Fossen, T.I., 1996. Design of a dynamic positioning system using model-based control. J. Control Eng. Pract. 4, 359–368.
Sørensen, A.J., Strand, J.P., Nyberg, H., 2002. Dynamic positioning of ships and floaters in extreme seas. In: Proceedings of the MTS-IEEE Conference (Oceans'02), Biloxi, Mississippi, US.
Strand, J.P., 1999. Nonlinear position control systems design for marine vessels (Ph.D. thesis). Department of Engineering Cybernetics, Norwegian University of Science and Technology, Trondheim, Norway.
Strand, J.P., Fossen, T.I., 1999. Nonlinear passive observer for ships with adaptive wave filtering. In: Nijmeijer, H., Fossen, T.I. (Eds.), New Directions in Nonlinear Observer

Design. Springer-Verlag London Ltd., pp. 113–134.
Torsetnes, G., Jouffroy, J., Fossen, T.I., 2004. Nonlinear dynamic positioning of ships with gain-scheduled wave filtering. In: Proceedings of the IEEE Conference on Decision and Control (CDC'04), Paradise Iceland, Bahamas.

Vasconcelos, J.F., Athans, M., Fekri, S., Silvestre, C., Oliveira, P., 2009. Stability- and performance-robustness tradeoffs: MIMO mixed-μ vs complex-μ design. Int. J. Robust. Nonlinear Control 19, 259–294.